A Comparison of Posterior Cramer–Rao Bounds for Point and Extended Target Tracking

Zhiwen Zhong, Huadong Meng, *Member, IEEE*, and Xiqin Wang

***Abstract*—This letter presents a theoretical comparative study of the performance bounds for point and extended target tracking. As a result of the additional information provided by the high-resolution sensors, the posterior Cramer–Rao lower bound (PCRLB) of the kinematic target states is proven to be always smaller under the extended target tracking framework than the point target model. Three assumptions about the two kinds of target models, which are satisfied in most target tracking problems, are presented as a sufficient condition of the inequality. This comparison result suggests the use of the extended target model to potentially achieve better performance in tracking applications. The superior performance bound is also illustrated with an elliptically modeled extended target tracking example.**

***Index Terms*—Elliptical target model, extended target tracking, posterior Cramer–Rao lower bound (PCRLB), tracking bound.**

I. Introduction

MOST conventional target tracking algorithms consider a target to be a single point source and estimate the target states through the incoming positional measurements of the target centroid. However, the point target model is no longer suitable for many cases because recent high-resolution sensors can resolve multiple point features on a single extended target. The use of high-resolution measurements is referred to as extended target tracking [2]–[4].

An extended target can be modeled as a rigid body, a semi-rigid body, or a set of point features. As a result of the complexity and nonlinearity of the extended target tracking model, the main focus of the extended target tracking problem is nonlinear filtering algorithms under various assumptions. In contrast to the point target tracking systems that only use the positional measurement of the target centroid, the extended measurements provided by high-resolution sensors, such as target extent, can provide extra information to improve target identification and data association [2].

Moreover, we will prove in this letter that the extended high-resolution measurements are not only able to provide new information, but also to improve the estimation accuracy of the conventional dynamic states of the target centroid, assuming that there is a correlation between the conventional target states and the new measurements. The posterior Cramer–Rao lower bound (PCRLB) provides a powerful tool to determine a bound on the optimal achievable accuracy of target state estimation. An efficient and general recursive formulation of the PCRLB has been derived in [1] and will be utilized in our derivation.

The tracking problem in our discussion does not concern the influence of missed detections and false alarms. However, the conclusion can be generalized directly to an environment with false alarms and missed detections by the Information Reduction Factor (IRF) [6], Measurement Sequence Conditioning (MSC) [7], and Measurement Existence Sequence Conditioning (MESC) [8] approaches.

Manuscript received April 28, 2010; revised July 07, 2010; accepted July 07, 2010. Date of publication July 19, 2010; date of current version August 09, 2010. This work was supported in part by the National Natural Science Foundation of China (60901057) and in part by the National Basic Research Program of China (973 Program, 2010CB731901). The associate editor coordinating the review of this manuscript and approving it for publication was Dr. Thia Kirubarajan.

The authors are with the Department of Electronic Engineering, Tsinghua University, Beijing 100084, China (e-mail: menghd@tsinghua.edu.cn).

Digital Object Identifier 10.1109/LSP.2010.2059699

II. Problem Statement

A. General State and Measurement Models

Let us consider the discrete-time, nonlinear filtering problem with additive Gaussian process and measurement noise. Let x (of dimensionality N_S) be the state vector and k be the time step; the state dynamic equation is given by

$$x_{k+1} = f_k(x_k) + q_k \tag{1}$$

where $f_k(\cdot)$ is the state transitional function which may be nonlinear, and q_k is zero-mean Gaussian noise with a nonsingular covariance matrix Q_k.

The measurement model we consider includes a single sensor and a single measurement vector (of dimensionality N_M) at each sampling time, which is formulated as

$$z_k = h_k(x_k) + r_k \tag{2}$$

where $h_k(x_k)$ is a (potentially) nonlinear function of the target state, and r_k is a zero-mean Gaussian measurement noise with a nonsingular covariance matrix R_k.

B. Recursive Form of the PCRLB

The closed form of the optimal solution of the nonlinear filtering problem defined by (1) and (2) is usually unachievable. However, the theoretically best achievable performance can be calculated in the form of the posterior Cramer–Rao lower bound (PCRLB).

Let $\hat{x}_k$ denote any unbiased estimator of x_k based on measurements $Z_k = \{z_1, \cdots z_k\}$; the covariance of $\hat{x}_k$ has a lower bound that is expressed as follows [5]:

$$C_k = E\left[(x_k - \hat{x}_k)(x_k - \hat{x}_k)^T\right] \geq J_k^{-1} \tag{3}$$

where J_k is referred to as the Fisher information matrix (FIM). The inverse J_k^{-1} is the PCRLB. The inequality in (3) means that the difference $C_k - J_k^{-1}$ is a non-negative definite matrix.

Tichavsky *et al.* [1] provided a Riccati-like recursion to calculate the FIM J_k. When the dynamic and measurement models are expressed by (1) and (2), respectively, the FIM is computed recursively as

$$J_{k+1} = J_Z(k+1) + Q_k^{-1} - Q_k^{-1}E[F_k]\left(J_k + E\left[F_k^T Q_k^{-1} F_k\right]\right)^{-1} E\left[F_k^T\right] Q_k^{-1} \quad (4)$$

where

$$J_Z(k+1) = E_{x_{k+1}}\left[H_{k+1}^T R_{k+1}^{-1} H_{k+1}\right] \quad (5)$$

is the measurement contribution, and F_k and H_k are the Jacobians of the nonlinear functions $f_k(x_k)$ and $h_k(x_k)$, i.e., $F_k = [\nabla_{x_k} f_k^T(x_k)]^T$, $H_k = [\nabla_{x_k} h_k^T(x_k)]^T$.

C. Point and Extended Target Tracking

To compare the performance bounds for different models, we denote the point and extended target model with the superscripts p and e, respectively. Thus, the state and measurement equations of the point and extended models are

$$x_{k+1}^p = f_k^p(x_k^p) + q_k^p, \quad z_k^p = h_k^p(x_k^p) + r_k^p \quad (6)$$

and

$$x_{k+1}^e = f_k^e(x_k^e) + q_k^e, \quad z_k^e = h_k^e(x_k^e) + r_k^e \quad (7)$$

respectively, where

$$q_k^p \sim N(0, Q_k^p), \quad r_k^p \sim N(0, R_k^p)$$
$$q_k^e \sim N(0, Q_k^e), \quad r_k^e \sim N(0, R_k^e). \quad (8)$$

The relationship between the two models obeys the following assumptions.

Assumption 1: The state vector of the point model is part of that of the extended model:

$$x^e = [x^p \quad x^n]^T. \quad (9)$$

The x^p component represents the conventional target states, such as the position and velocity of the target centroid, and the extended part x^n is the additional state of the extended target, such as the target size and shape.

Assumption 2: The evolution of the conventional part of the extended target state is the same as that of the point model and is hence independent of the additional part, i.e.,

$$f_k^e(x^e) = [f_k^p(x^p) \quad f_k^n(x^e)]^T, \quad (10)$$
$$\Gamma[Q_k^e] = Q_k^p \quad (11)$$

where $\Gamma(\cdot)$ is a function to obtain the $N_S^p \times N_S^e$ left-upper submatrix. The initial FIMs of both models also obey the submatrix relationship:

$$J_0^e = diag(J_0^p, J_0^n). \quad (12)$$

Assumption 3: The measurement equation of the extended target model is also an extension of that of the point target model. Meanwhile, the new measurement is correlated with the conventional target states, and the conventional measurement is independent of the extended measurements:

$$h_k^e(x^e) = [h_k^p(x^p) \quad h_k^n(x^e)]^T, \quad R_k^e = diag(R_k^p, R_k^n) \quad (13)$$

and

$$\frac{\partial h_k^p(x^p)}{\partial x^n} = 0, \quad \frac{\partial h_k^n(x^e)}{\partial x^p} \neq 0. \quad (14)$$

As a result, the additional measurements can provide extra information about the conventional target states.

In most of the extended target tracking frameworks [2]–[4], the tracking model consists of target centroid kinematics and parameters of target extension, completely satisfying the three assumptions presented above.

III. Comparison of the PCRLBs

A. PCRLBs of Point and Extended Models

The FIMs of point and extended target tracking, denoted as J_k^p and J_k^e, can be calculated recursively. We prove that the left-upper submatrix (of dimensionality $N_S^p \times N_S^p$) of $(J_k^e)^{-1}$ is always less than $(J_k^p)^{-1}$, which suggests that we can potentially obtain better tracking performance by constructing the extended target model with the additional measurements. The problem can be written as

$$\Gamma\left[(J_k^e)^{-1}\right] < (J_k^p)^{-1}. \quad (15)$$

B. The Self-Defined Model

Calculating the left-upper submatrix of the PCRLB of (15) is quite inconvenient. To illustrate the influence of the new measurements, we define another extended target tracking model (denoted as superscript d), which has the same state space and dynamic equation as the extended target model "e", and the same measurement equation as the point target model "p"; the self-defined model is written as

$$x_{k+1}^d = f_k^e(x_k^d) + q_k^d, \quad (16)$$
$$z_k^d = h_k^p(x_k^p) + r_k^d \quad (17)$$

where $x^d = x^e$, $q_k^d \sim N(0, Q_k^e)$, $r_k^d \sim N(0, R_k^p)$, and the initial FIM $J_0^d = J_0^e$.

C. Relationship Between the PCRLBs

Note that the extended part of the target state of the defined model evolves totally independently; hence, the conventional target state evolution is completely the same as that of the point target model. Thus, the left-upper $N_S^p \times N_S^p$ submatrix of $(J_k^d)^{-1}$ is always equal to $(J_k^p)^{-1}$:

$$\Gamma\left[\left(J_k^d\right)^{-1}\right] = (J_k^p)^{-1}. \quad (18)$$

Thus, (15) is equivalent to

$$\Gamma\left[(J_k^e)^{-1}\right] < \Gamma\left[\left(J_k^d\right)^{-1}\right]. \quad (19)$$

Intuitively, from model "d" to model "e," the estimation accuracy should be improved entirely with the help of the extended measurements:

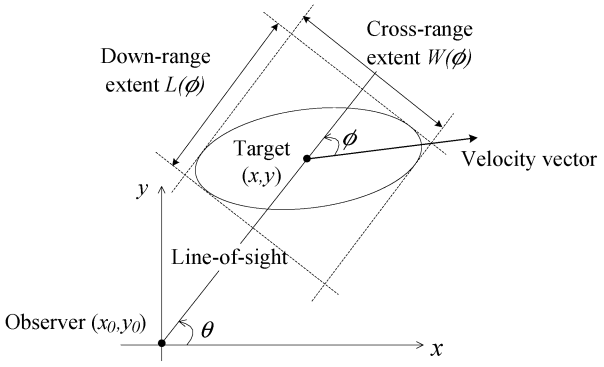

Fig. 1. Elliptical model for extended target.

$$\left(J_k^e\right)^{-1} < \left(J_k^d\right)^{-1}. \tag{20}$$

The proof of (20) is given in the Appendix, and (19) is a direct inference.

IV. An Extended Target Tracking Example

The previous theoretical result is illustrated here in an example of tracking an extended target that is modeled by an ellipse [2], [4]. The radar sensor obtains the measurement of the extent of the target along the line-of-sight (LOS) and perpendicular to the LOS, in addition to the conventional position measurement of the target centroid, as shown in Fig. 1.

The target is moving with nearly constant velocity (NCV), and the point tracking model is of the conventional form:

$$x_{k+1}^p = F_k^p x_k^p + q_k^p, \tag{21}$$

$$z_k^p = h_k^p\left(x_k^p\right) + r_k^p = \left[\rho\left(x_k^p\right) \quad \theta\left(x_k^p\right)\right]^T + r_k^p \tag{22}$$

where $x_k^p = (x, \dot{x}, y, \dot{y})_k^T$, $F_k^p = diag\left(\begin{bmatrix}1 & T\\ 0 & 1\end{bmatrix}, \begin{bmatrix}1 & T\\ 0 & 1\end{bmatrix}\right)$, $\rho(x^p) = \sqrt{(x-x_0)^2+(y-y_0)^2}$, $\theta(x^p) = \arctan((y-y_0)/(x-x_0))$, and T is the time interval between measurements.

The state vector of the extended target tracking problem is extended to $x_k^e = (x, \dot{x}, y, \dot{y}, l, \gamma)_k^T$, where l and γ are the length of the main axis and the aspect ratio of the ellipse, respectively. The dynamic and measurement models of the problem are

$$x_{k+1}^e = F_k^e x_k^e + q_k^e \tag{23}$$

and

$$z_k^e = h_k^e\left(x_k^e\right) + r_k^e \tag{24}$$

where $F_k^e = diag(F_k^p, I_2)$, $h_k^e(x^e)$ is composed of two parts, as defined in (13), and $h_k^n(x^e)$ is dependent on both the conventional target states and the extended target states:

$$h_k^n(x^e) = \begin{bmatrix}L(\phi)\\ W(\phi)\end{bmatrix} = \begin{bmatrix}l\sqrt{\cos^2\phi + \gamma^2\sin^2\phi}\\ l\sqrt{\sin^2\phi + \gamma^2\cos^2\phi}\end{bmatrix} \tag{25}$$

where $L(\phi)$ and $W(\phi)$ are the down-range and cross-range extent of the target, respectively, and ϕ is the angle between the LOS and the velocity vector, denoted as the VLOS angle:

$$\phi = \arctan\left[\frac{\dot{x}(y-y_0) - \dot{y}(x-x_0)}{\dot{x}(x-x_0) + \dot{y}(y-y_0)}\right]. \tag{26}$$

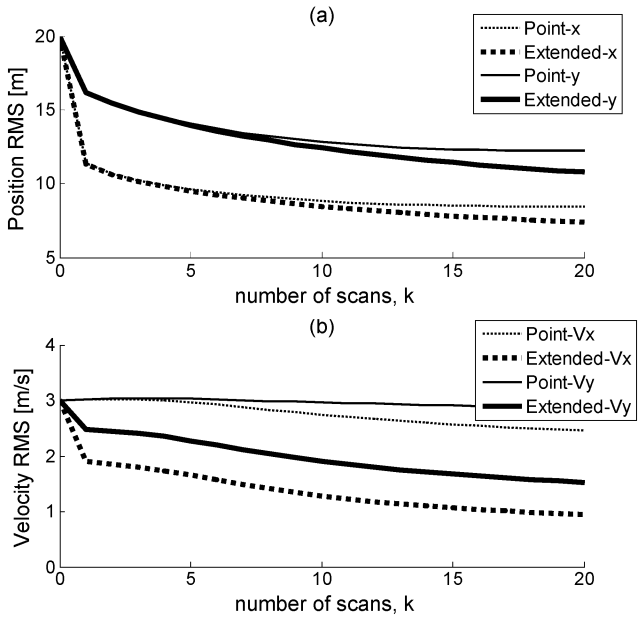

Fig. 2. Comparisons of PCRLBs using the point and extended target models for (a) position (x, y) and (b) velocity $(\dot{x}, \dot{y})$.

In our simulation, the observer is static and at the origin of the coordinate system, while the target moves with initial velocity $v_0 = 10$ in the direction with the VLOS angle $\phi_0 = 20°$. The initial position of the target is (15 000, 10 000). The parameters of the ellipse are $l = 50$ and $\gamma = 0.2$. The initial FIM is $J_0^e = diag(20, 3, 20, 3, 5, 0.1)^2$. The covariance of the state noise is $Q_k^e = diag(3, 0.1, 3, 0.1, 1, 10^{-4})$, and the measurement noise is zero-mean white Gaussian noise with standard deviations: $\sigma_\rho = 5$, $\sigma_\theta = 0.2°$, $\sigma_L = 3$, and $\sigma_W = 3$. The time interval is $T = 0.2$. All the parameter units are in the metric system.

The PCRLB is calculated using the recursion (4). As shown in Fig. 2, the tracking PCRLBs of the position and the velocity of the target centroid using the extended model are always less than the ones found using the point target model.

In Fig. 2(b), the PCRLBs of the velocities of the extended target model in both the x and y directions decrease sharply upon the arrival of the measurements (the initial values are equivalent). The improvement in the bound is a result of the measurements of target extent being dependent on the target velocity.

V. Conclusion

This letter presented a theoretical comparison of the tracking performance bound of target centroid dynamics under point and extended target models. The PCRLB of the conventional target states was proven to be always smaller with the extended target model by assuming that the extended target states and measurements are extensions of those of the point target (the conventional parts of the target states and measurements of the two models are the same), and the new measurements are correlated to the conventional target states.

The theoretical result reveals that the extended target tracking framework could potentially improve the tracking accuracy of the dynamic states of the target centroid with the information

provided by high-resolution sensors. The conclusion was also verified on a common extended target tracking example.

APPENDIX

We prove the result by induction. We will show that

$$\left(J_k^e\right)^{-1} \le \left(J_k^d\right)^{-1} \Rightarrow \left(J_{k+1}^e\right)^{-1} < \left(J_{k+1}^d\right)^{-1}, \quad k \ge 0. \tag{27}$$

For convenience, we define A_k and B_{k+1} as

$$A_k = Q_k^{-1} - Q_k^{-1}E[F_k]\left(J_k + E\left[F_k^T Q_k^{-1} F_k\right]\right)^{-1} \times E\left[F_k^T\right] Q_k^{-1} \tag{28}$$

$$B_{k+1} = (H_{k+1})^T (R_{k+1})^{-1} H_{k+1}. \tag{29}$$

Hence, the PCRLBs for model "e" and "d" are written as

$$J_{k+1}^e = A_k^e + E\left[B_{k+1}^e\right], \tag{30}$$

$$J_{k+1}^d = A_k^d + E\left[B_{k+1}^d\right]. \tag{31}$$

We denote

$$Q_k = Q_k^e = Q_k^d, \quad F_k = F_k^e = F_k^d. \tag{32}$$

It follows from the inductive statement (27) that

$$Q_k^{-1}E[F_k]\left(J_k^e + E\left[F_k^T Q_k^{-1} F_k\right]\right)^{-1} E\left[F_k^T\right] Q_k^{-1} \le Q_k^{-1}E[F_k]\left(J_k^d + E\left[F_k^T Q_k^{-1} F_k\right]\right)^{-1} E\left[F_k^T\right] Q_k^{-1} \tag{33}$$

and then we can obtain

$$A_k^e \ge A_k^d. \tag{34}$$

On the other side, the measurement contributions of the two models are defined as

$$B_{k+1}^e = \left(H_{k+1}^e\right)^T \cdot \begin{bmatrix} \left(R_{k+1}^p\right)^{-1} & 0 \\ 0 & \left(R_{k+1}^n\right)^{-1} \end{bmatrix} \cdot H_{k+1}^e \tag{35}$$

and

$$B_{k+1}^d = \left(H_{k+1}^d\right)^T \cdot \left(R_{k+1}^p\right)^{-1} \cdot H_{k+1}^d \tag{36}$$

where the Jacobians can be calculated as (from Assumption 3)

$$H_{k+1}^e = \begin{bmatrix} \frac{\partial h_{k+1}^p\left(x_{k+1}^p\right)}{\partial x_{k+1}^p} & \frac{\partial h_{k+1}^p\left(x_{k+1}^p\right)}{\partial x_k^n} \\ \frac{\partial h_k^n\left(x_k^e\right)}{\partial x_k^p} & \frac{\partial h_{k+1}^n\left(x_{k+1}^e\right)}{\partial x_{k+1}^n} \end{bmatrix} = \begin{bmatrix} H_{k+1}^p & 0 \\ H_{k+1}^3 & H_{k+1}^4 \end{bmatrix} \tag{37}$$

and

$$H_{k+1}^d = \begin{bmatrix} \frac{\partial h_{k+1}^p\left(x_{k+1}^p\right)}{\partial x_{k+1}^p} & \frac{\partial h_{k+1}^p\left(x_{k+1}^p\right)}{\partial x_{k+1}^n} \end{bmatrix} = \begin{bmatrix} H_{k+1}^p & 0 \end{bmatrix}. \tag{38}$$

Thus we can then obtain

$$B_{k+1}^e = \begin{bmatrix} \left(H_{k+1}^3\right)^T \\ \left(H_{k+1}^4\right)^T \end{bmatrix} \left(R_{k+1}^n\right)^{-1} \begin{bmatrix} H_{k+1}^3 & H_{k+1}^4 \end{bmatrix} + \begin{bmatrix} \left(H_{k+1}^p\right)^T \left(R_{k+1}^p\right)^{-1} H_{k+1}^p & 0 \\ 0 & 0 \end{bmatrix} \tag{39}$$

and

$$B_{k+1}^d = \begin{bmatrix} \left(H_{k+1}^p\right)^T \left(R_{k+1}^p\right)^{-1} H_{k+1}^p & 0 \\ 0 & 0 \end{bmatrix}. \tag{40}$$

It then follows from (39) and (40) that

$$B_{k+1}^e - B_{k+1}^d = \begin{bmatrix} \left(H_{k+1}^3\right)^T \\ \left(H_{k+1}^4\right)^T \end{bmatrix} \left(R_{k+1}^n\right)^{-1} \begin{bmatrix} H_{k+1}^3 & H_{k+1}^4 \end{bmatrix} > 0 \quad \text{for all } x_{k+1}. \tag{41}$$

Hence,

$$J_Z^e(k+1) > J_Z^d(k+1). \tag{42}$$

From (30), (31), (34), and (42), we can show that

$$J_{k+1}^e > J_{k+1}^d \tag{43}$$

and therefore

$$\left(J_{k+1}^e\right)^{-1} < \left(J_{k+1}^d\right)^{-1}. \tag{44}$$

Note that the initial FIMs for both model "e" and "d" are the same ($J_0^e = J_0^d$), so (20) holds for all $k > 0$.

ACKNOWLEDGMENT

The authors would like to thank Dr. M. L. Hernandez for providing professional comments about the problem discussed in this letter.

REFERENCES

[1] P. Tichavsky, C. Muravchik, and A. Nehorai, "Posterior Cramer–Rao lower bounds for discrete-time nonlinear filtering," *IEEE Trans. Signal Process.*, vol. 46, no. 5, pp. 1386–1396, May 1998.

[2] D. J. Salmond and M. C. Parr, "Track maintenance using measurements of target extent," *Proc. Inst. Elect. Eng., Radar Sonar Navig.*, vol. 150, no. 6, Dec. 2003.

[3] K. Gilholm and D. Salmond, "Spatial distribution model for tracking extended objects," *Proc. Inst. Elect. Eng., Radar Sonar Navig.*, vol. 152, no. 5, pp. 364–371, 2005.

[4] D. Angelova and L. Mihaylova, "Extended object tracking using monte carlo methods," *IEEE Trans. Signal Process.*, vol. 56, no. 2, pp. 825–832, Feb. 2008.

[5] H. van Trees, *Detection, Estimation, and Modulation Theory*. New York: Wiley, 1968.

[6] X. Zhang, P. Willett, and Y. Bar-Shalom, "Dynamic Cramer–Rao bound for target tracking in clutter," *IEEE Trans. Aerosp. Electron. Syst.*, vol. 41, no. 4, pp. 1154–1167, 2005.

[7] M. L. Hernandez, A. Farina, and B. Ristic, "PCRLB for tracking in cluttered environments: Measurement sequence conditioning approach," *IEEE Trans. Aerosp. Electron. Syst.*, vol. 42, no. 2, pp. 680–704, 2006.

[8] H. Meng, M. L. Hernandez, Y. Liu, and X. Wang, "Computationally efficient PCRLB for tracking in cluttered environments: Measurement existence conditioning approach," *IET Signal Process.*, vol. 3, no. 2, pp. 133–149, Mar. 2009.